Available online at www.sciencedirect.com
ScienceDirect
Carbohydrate Research 342 (2007) 724–735
Carbohydrate RESEARCH

Structure elucidation of arabinoxylan isomers by normal phase HPLC–MALDI-TOF/TOF-MS/MS

Sarah L. Maslen,[a] Florence Goubet,[b,†] Alex Adam,[c] Paul Dupree[b] and Elaine Stephens[a,*]

[a]*Department of Chemistry, University of Cambridge, Lensfield Road, Cambridge CB2 1EW, UK*
[b]*Department of Biochemistry, Building O, Downing Site, Cambridge CB2 1QW, UK*
[c]*Dionex UK Ltd, 4 Albany Court, Albany Industrial Estate, Camberley, Surrey, GU16 7QL, UK*

Received 7 September 2006; received in revised form 16 November 2006; accepted 11 December 2006
Available online 15 December 2006

Abstract—Normal phase-high performance liquid chromatography (NP-HPLC) coupled to matrix-assisted laser desorption/ionization-time-of-flight/time-of-flight (MALDI-TOF/TOF) tandem mass spectrometry is evaluated for the detailed structural characterization of various isomers of arabinoxylan (AX) oligosaccharides produced from endo-β-(1→4)-xylanase (endoxylanase) digestion of wheat AX. The fragmentation characteristics of these oligosaccharides upon MALDI-TOF/TOF high-energy collision induced dissociation (CID) were investigated using purified AX oligosaccharide standards labeled at the reducing end with 2-aminobenzoic acid (2-AA). A variety of cross-ring cleavages and 'elimination' ions in the fragment ion spectra provided extensive structural information, including Ara*f* substitution patterns along the xylan backbone and comprehensive linkage assignment. The off-line coupling of this MALDI-CID technique to capillary normal phase HPLC enabled the separation and identification of isomeric oligosaccharides (DP 4–8) produced by endoxylanase digestion of AX. Furthermore, this technique was used to characterize structurally different isomeric AX oligosaccharides produced by endoxylanase enzymes with different substrate specificities.

Keywords: MALDI-TOF/TOF; Arabinoxylan; Isomers; High-energy CID; Normal phase HPLC

1. Introduction

Arabinoxylans (AX) are the main polysaccharides found in the cereal cell wall. They are comprised of a linear β-(1→4)-linked xylopyranose (Xyl*p*) backbone substituted with arabinofuranose (Ara*f*) side chains attached via α-(1→3) and/or α-(1→2) linkages.[1] AX purified from various cereals or tissues have the same fundamental chemical structures although different Ara/Xyl ratios have been reported.[1] There is a high degree of heterogeneity associated with these polysaccharides, which prevents the complete structure elucidation of one single structure. This heterogeneity is caused by variation in the degree of polymerization (DP) and branching, the distribution of Ara*f* residues along the xylan backbone and the proportion of the different types of linkage of the Ara*f* residues in the Xyl*p* ring. These structural differences are responsible for the variations in the physiochemical and biological properties of the arabinoxylans.[1]

The fine structure of these heterogeneous compounds has been determined by NMR analyses of AX oligosaccharides produced from endoxylanase digestion.[2–4] This method requires purified and homogeneous samples in micromole/nanomole quantities and, although information regarding the amount and type of specific linkages and overall configuration can be acquired, sequence information is not obtained. Therefore, mass spectrometry (MS) in combination with NMR, has been employed for complete characterization.[5–7] Modern mass spectrometric methods are capable of providing extensive oligosaccharide structural information including carbohydrate composition, branching, and sometimes linkage information in the low picomole-femtomole range. However, after endoxylanase digestion, the structures of the AX oligosaccharides are notoriously difficult

* Corresponding author. Tel.: +44 1223 763126; fax: +44 1223 336913; e-mail: es287@cam.ac.uk
† Present address: Bayer BioScience N.V., Technologiepark 38, B-9052 Zwijnaarde, Belgium.

0008-6215/$ - see front matter © 2006 Elsevier Ltd. All rights reserved.
doi:10.1016/j.carres.2006.12.007

to determine by MS alone because Ara*f* and Xyl*p* have the same molecular weight (pentose) and many isobaric structural isomers are present.

Recently, an ESI-ITMS approach has successfully identified structural isomers of permethylated AX oligosaccharides produced by endoxylanase digestion of wheat AX.[8,9] The presence of isomeric components containing up to six monosaccharide residues was demonstrated using multiple ESIMS^n experiments. However, linkage information could not be fully obtained using this technique and the analysis of partially methylated alditol acetates by GC–MS was required.[9] Another very recent study has employed negative ion ESI-Q-TOF CID to decipher the structures of purified native mono- and disubstituted AX oligosaccharides (up to DP 9) that were previously characterized by ^{1}H NMR.[10] Using this ESI method, the substitution patterns of various reducing-end ^{18}O-labeled oligosaccharides could be assigned and partial linkage information was obtained from ^{0,2}A cross-ring fragments.

In the past few years MALDI-TOF/TOF tandem mass spectrometry has been shown to provide extensive oligosaccharide structural information. MALDI high-energy CID spectra of both positive and negative molecular ions provide sequence, branching, and linkage information.[11–14] Particularly abundant fragment ions are the 'elimination' and cross-ring fragments, which give important linkage and branching information. In addition, this mass spectrometric method has the ability to identify structural isomers.[11,13,15] Therefore, the coupling of this technique to HPLC methods that are able to separate isobaric oligosaccharide components should enable extensive structure elucidation of complex mixtures. Recently, normal phase (NP) HPLC has been shown to differentiate some isobaric *N*-glycans.[16,17] In NP-HPLC, retention is caused by polar interactions, which generally increase with elongation of the oligosaccharide chains, and often allows some prediction of elution positions. This chromatographic technique is known to be very useful in the analysis of fluorescently labeled *N*-glycans, and has frequently been employed on an analytical or microbore scale to separate labeled glycans with fluorescence detection followed by analysis by mass spectrometry.[18–20]

In this study, off-line NP-HPLC–MALDI-TOF/TOF tandem mass spectrometry is evaluated for the structural characterization of a heterogeneous mixture of AX oligosaccharides. The MALDI-CID fragmentation characteristics of AX standards reductively aminated with a UV-absorbing tag (2-aminobenzoic acid, 2-AA) is determined. Cross-ring fragments and 'elimination' ions in the high-energy spectra provide very detailed structural information on sequence, branching, and linkage. Subsequent NP-HPLC–MALDI-TOF/TOF-MS/MS experiments on reducing-end labeled AX oligosaccharides, produced from endoxylanase digestions, show that this method is capable of separating AX structural isomers, which are identified by specific fragment ions in the fragment ion spectra. This powerful NP-HPLC–MALDI-TOF/TOF method is employed to investigate the enzyme specificities of two endoxylanase enzymes from glycosyl hydrolase (GH) family 10 and family 11 (CAZy database[21–23]), where structural differences in the AX chains were differentiated by their retention time in the NP chromatography and by key fragment ions in the MALDI-CID spectra.

2. Results and discussion

2.1. MALDI-TOF-MS analyses of AX oligosaccharide mixtures produced by digestion with two different endoxylanases

MALDI-TOF/TOF tandem mass spectrometry was first employed for the direct analyses of AX oligosaccharide isomeric mixtures produced by digestion of wheat arabinoxylan with endo-β-(1→4)-xylanases from two different GH families: GH 10 or GH 11. One fundamental difference between these two major families is that the GH 11 xylanases digest relatively unsubstituted regions of xylan, whereas some family 10 enzymes are able to hydrolyze decorated forms of the polysaccharide backbone.[24] The oligosaccharides produced by endoxylanase digestion were reductively aminated with 2-AA for two reasons: (1) to provide a chromophore for detection of the oligosaccharides by NP-HPLC experiments and (2) to differentiate between reducing- and non-reducing end fragments formed upon MALDI-CID. Initial experiments involved the direct analyses of the 2-AA labeled digestion mixtures by MALDI-TOF-MS where a series of molecular ions ($[M+H]^+$, $[M+Na]^+$, and $[M-H+2Na]^+$) are observed for each oligomer from DP 4 to DP 15 (Fig. 1). Comparison of the molecular ion profiles of each sample revealed that larger molecular weight oligosaccharides ($\geqslant$DP 5) were more abundant in the GH 11 xylanase enzyme preparation. These data are not surprising as previous studies have shown that the GH 10 enzyme produces smaller oligosaccharides than the endoxylanase from GH family 11.[24] Subsequent MALDI-CID experiments on chosen $[M+Na]^+$ molecular ions gave fragment ion spectra, which were difficult to interpret due to the presence of structural isomers (data not shown). Therefore, each heterogeneous sample was subjected to off-line NP-HPLC–MALDI-TOF/TOF tandem mass spectrometry for more extensive structural characterization.

2.2. NP-HPLC–MALDI-TOF/TOF analyses of AX standards

Prior to analyses of endoxylanase digested wheat AX, NP-HPLC–MALDI-TOF/TOF-MS/MS was first

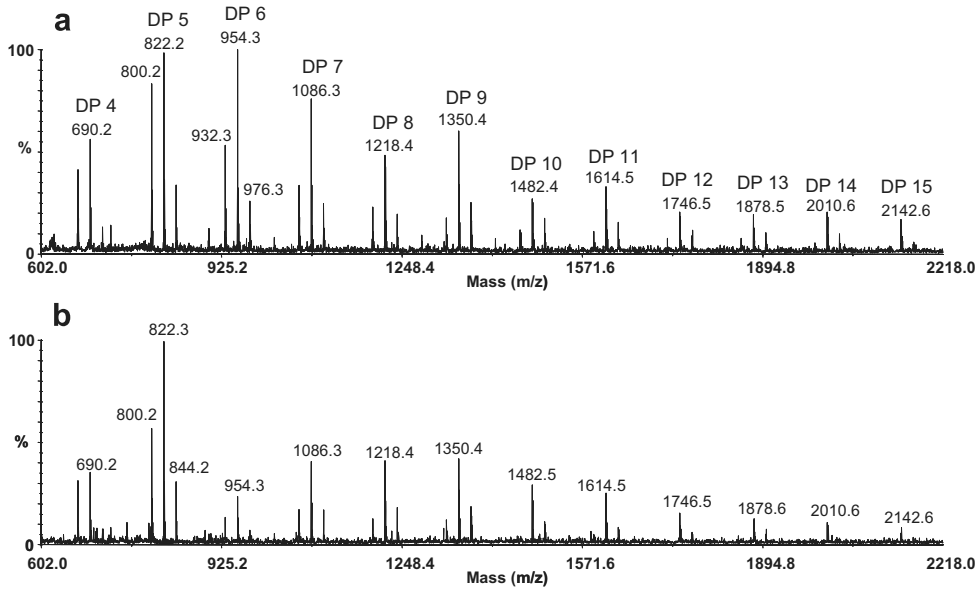

Figure 1. MALDI-TOF-MS spectra showing signals ($[M+H]^+$, $[M+Na]^+$, and $[M-H+2Na]^+$) for the 2-AA labeled oligosaccharides produced from digestion of wheat AX with endoxylanase from GH family (a) 11 and (b) 10. The major signals (corresponding to $[M+Na]^+$) in each cluster are labeled with the pentose oligomers (DP 4–DP 15).

evaluated for the separation and structure elucidation of two AX standard oligosaccharides (DP 5 and DP 6) reductively aminated with 2-AA (extracted ion chromatograms are shown in Fig. 2). Co-chromatography with oligomeric glucose units in a dextran ladder (labeled with aminobenzamide (2-AB)) allowed the determination of retention properties in a standardized manner and facilitated the direct comparison of these AX standards with subsequent AX samples. The NP-HPLC–MALDI-CID spectra of the 2-AA labeled DP 5 and DP 6 AX standards are shown in Figure 3a and b, respectively. The series of cross-ring ^{1,5}X ions in these spectra give crucial sequence information showing the distribution of the Ara*f* along the xylan backbone. The non-reducing ^{3,5}A ions confirm this sequence assignment and also indicate the presence of (1→4) glycosidic linkages. More linkage information is provided by the series of ^{0,2}X ions, which reveal Ara*f* substitution at the C-2 position in the xylan backbone (Fig. 3b). Abundant E ions (according to the nomenclature introduced by Spina et al.[12], see Scheme 1a) confirm this linkage assignment as these ions are formed by the elimination of the substituent (e.g., Ara*f* or OH) at the C-2 position of the reducing-end residue in the corresponding B ion. Other major 'elimination' ions (G, D, and F, whose structures are shown in Scheme 1) show the presence of Ara*f* at the C-3 position of Xyl*p*. These ion types are abundant in MALDI-CID spectra of *N*-glycans and human milk oligosaccharides where the sugar moieties at the C-3 position can be clearly defined.[12,13,25] Other major ions at *m*/*z* 556.3 (Fig. 3a) and *m*/*z* 688.3 (Fig. 3b) correspond to the double cleavages, Y_3 and

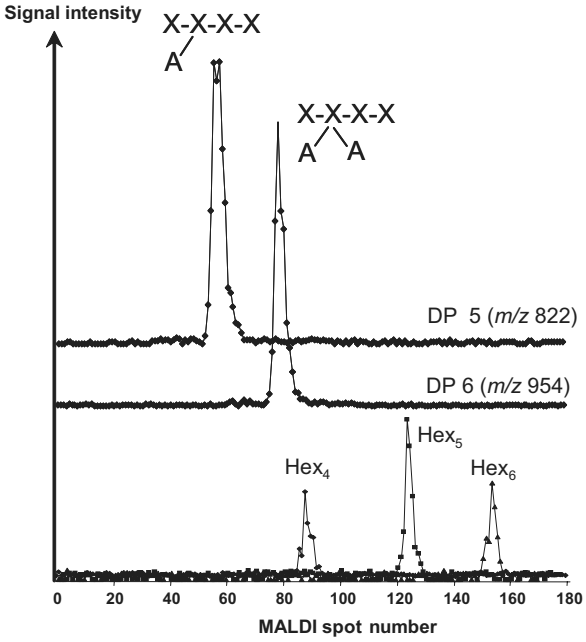

Figure 2. Capillary NP-HPLC–MALDI-TOF-MS of AX oligosaccharides standards labeled with 2-AA with the addition of the dextran ladder (labeled with 2-AB). The extracted ion chromatograms of DP 5 ($AraXyl_4$; *m*/*z* 822 $[M+Na]^+$) and DP 6 (Ara_2Xyl_4; *m*/*z* 954 $[M+Na]^+$) are shown along with the superimposed extracted ion chromatograms of the glucose oligomers in the dextran ladder (indicated by Hex_4–Hex_6). Symbol representation of AX structure is: Ara*f*, A; Xyl*p*, X; (1→4)linkage, –; (1→3)linkage, /; (1–2)linkage, \.

$Y_{3\alpha}$, along with the complete loss of two protons to result in the formation of a sugar lactone. The proposed

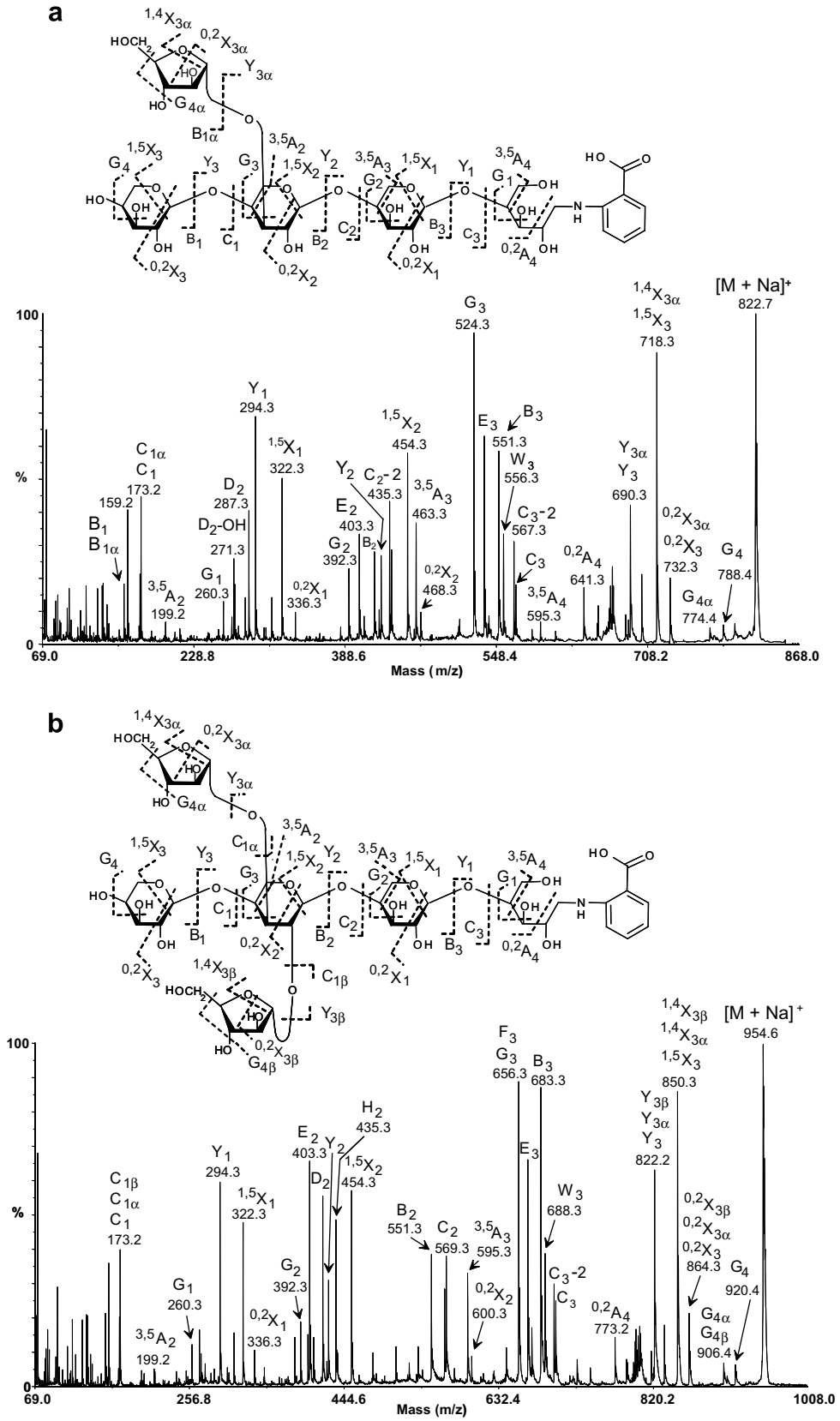

Figure 3. NP-HPLC–MALDI-CID of AX oligosaccharide standards. Chemical structures and CID spectra of (a) DP 5 ($AraXyl_4$) and (b) DP 6 (Ara_2Xyl_4). Glycosidic and cross-ring fragments are identified according to Domon and Costello nomenclature.[31] The proposed structures of the major ions denoted D, E, F, and G (nomenclature by Harvey[25] and Spina et al.[12]), H and W ions are summarized in Scheme 1.

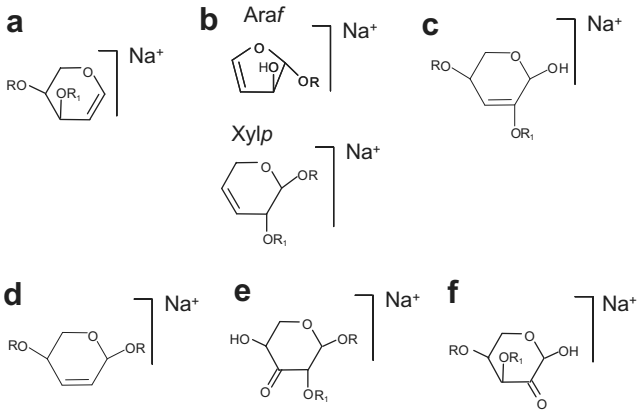

Scheme 1. Proposed chemical structures for the 'elimination' ions observed in all MALDI-CID spectra of AX oligosaccharides: (a) E ion,[12] (b) G ions (for Ara*f* and Xyl*p*),[12] (c) D ion,[25] (d) F ion,[12] (e) W ion and (f) H ion. R = xylan backbone and R_1 = Ara*f*.

structures for these reducing end ions (denoted W ions) are shown in Scheme 1e. Importantly, these lactone-forming double cleavages, which incorporate the reducing end, are observed only when Ara*f* is 3-linked to the xylan backbone. Interestingly, a corresponding non-reducing end fragment (denoted H_2; Scheme 1f) is seen only when Ara*f* is 2-linked to Xyl*p* (see Fig. 3b at *m*/*z* 435.3). The assigned structures of all these diagnostic ions were corroborated by MALDI-CID of the 2-aminobenzamide (2-AB) labeled and permethylated standard AX oligosaccharides, where their *m*/*z* values shifted accordingly (data not shown). The sugar lactone fragments shown in Scheme 1e and f provide a plausible and convenient rationalization of the observed masses, but in the absence of isotope labeling experiments other formalizations are possible. Together with the abundant cross-ring and glycosidic fragmentation, these 'elimination' ions (E, G, D, and F) and 'sugar lactone' (H and W) ions provide extensive structural information of purified AX oligosaccharides.

2.3. NP-HPLC–MALDI-TOF/TOF tandem mass spectrometric analyses of AX isomers produced by digestion with different endoxylanases

Isomeric mixtures of AX oligosaccharides, produced by digestion of wheat AX with two different endoxylanase enzymes (from GH family 10 and 11), were analyzed using this normal phase method. Co-chromatography of both GH 10 and GH 11 oligosaccharide samples with a dextran ladder allowed direct comparisons between the different samples and the AX standards. The extracted ion chromatograms of DP 4–6 in the endoxylanase GH 11 digestion mixture are shown in Figure 4a, where the presence of structural isomers is apparent in oligosaccharides DP 5, DP 6. The direct comparison of these data with the extracted ion chromatograms of oligosaccharides with the same DPs in the GH 10 xylanase preparation (Fig. 4b) showed that some isomeric components have different elution times. For example, the DP 4 isomer, produced from GH 11 digestion, eluted later in the NP chromatography than its GH 10 counterpart. Together, these data suggest that the endoxylanases have produced some structurally different AX polymers.

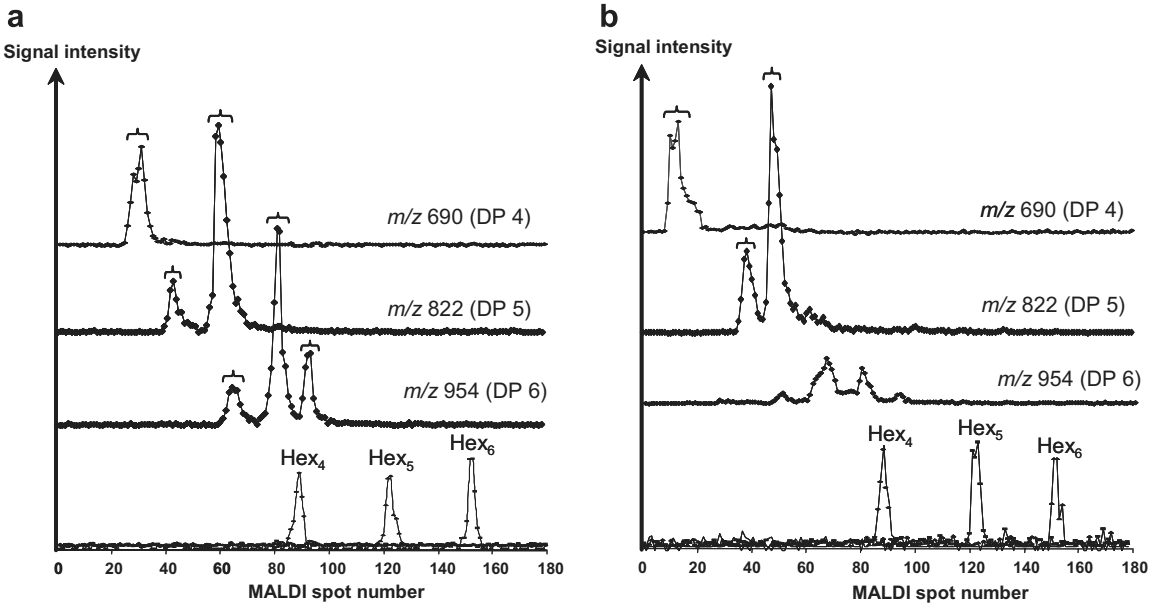

Figure 4. Capillary NP-HPLC–MALDI-TOF-MS of 2-AA labeled AX oligosaccharides produced by enzyme digestion with endoxylanase (a) from GH family 11 and (b) GH family 10. The extracted ion chromatograms of DP 4 (*m*/*z* 690 $[M+Na]^+$), DP 5 (*m*/*z* 822 $[M+Na]^+$), and DP 6 (*m*/*z* 954 $[M+Na]^+$) are shown along with the superimposed extracted ion chromatograms of the glucose oligomers in the dextran ladder (indicated by Hex_4–Hex_6). MALDI-CID spectra of selected $[M+Na]^+$ ions were accumulated across regions indicated by curly brackets.

The detailed structures of these small isomeric components (DP 4–DP 6) were determined by high-energy CID. The resulting fragmentation spectra of DP 4 (m/z 690 $[M+Na]^+$) produced from GH 11 and GH 10 hydrolysis (shown in Fig. 5a and b, respectively) exhibited fragment ions, which revealed structurally different oligosaccharides. The $^{1,5}X_1$ ion in both spectra showed that the derivatized (2-AA labeled) reducing-end Xyl*p* is not linked to Ara*f* in both oligomers. The significant $^{0,2}X_1$ ion (m/z 336.3) in the GH 11 oligosaccharide (Fig. 5a) indicates that position C-2 in the middle Xyl*p* is also not substituted with Ara*f*. This is supported by the dominant E_2 ion at m/z 403.3, which is formed by elimination of OH from the C-2 position of the B_2 ion. The absence of these ions (at m/z 336.3 and 403.3) in the MALDI-CID spectrum of the GH 10 isomer (Fig. 5b) and the concomitant appearance of a minor signal at m/z 468.3 ($^{0,2}X_1$) indicates that the 2-position of non-reducing end Xyl*p* is linked to Ara*f*. The presence of this C-2 branching substituent is supported by the major ion at m/z 303.3 (H_2). This so-called H-type non-reducing fragment (observed upon MALDI-CID of AX standard oligosaccharides (see Fig. 3b)) is only seen when Ara*f* is attached to Xyl*p* via C-2. The presence of unsubstituted Xyl*p* at the non-reducing end in the oligosaccharide produced by endoxylanase from GH family 11 is shown by the minor cross-ring $^{3,5}A_2$ ion at m/z 199.2 and the key elimination ion G_3 at m/z 656.4 (see Fig. 5a). Importantly, these ions are absent in Figure 5b and the appearance of a new G_2 ion (m/z 524.3) indicates that Ara*f* is linked to the 3-position of Xyl*p* at the non-reducing end of the GH 10 derived oligosaccharide. These data show that the endoxylanase from GH 11 produces oligosaccharides with unsubstituted Xyl*p* at the reducing- and non-reducing ends. By comparison, the GH 10 xylanase hydrolyses AX to give oligomers with substituted Xyl*p* at the non-reducing end. These structural data are consistent with the known enzyme specificities of GHs from family 10 and 11.[24,26]

The extracted ion chromatograms of the DP 5 oligosaccharides (m/z 822 $[M+Na]^+$) from both GH 10 and 11 digestions showed very similar profiles (Fig. 4a and b), indicating that the same oligosaccharides may be present. However, MALDI-CID of all four putative isomeric components gave very distinct fragment ions that identified different oligomers. Two resolved peaks containing isobaric AX oligosaccharides (DP 5) were observed from GH 11 digestion (Fig. 4a). The minor isomer eluted earlier than its more abundant counterpart and gave high-energy fragment ions upon MALDI-CID (Fig. 6a), which indicated that this oligosaccharide is disubstituted with Ara*f* on the middle Xyl*p* residue (Ara_2Xyl_3). The other more abundant isobaric structure eluted at the same position as the $AraXyl_4$ (DP 5) standard (compare Figs. 2 and 4) and gave an identical fragment ion spectrum (shown in Fig. 6b). Therefore, this isomer was assigned to the monosubstituted oligomer ($AraXyl_4$) with Ara*f* 3-linked to the penultimate Xyl*p* at the non-reducing end. Diagnostic fragment ions (e.g., a $^{1,5}X$ ion at m/z 586) for the other possible isobaric structure (containing Ara*f* 3-linked to the penultimate Xyl*p* residue at the reducing end), were not observed in any of the NP-HPLC–MALDI-CID data. Consequently, this isobaric oligosaccharide was presumed not to be present at a detectable level.

Hydrolysis of wheat AX with xylanase of GH 10 also gave two main peaks for DP 5 (m/z 822 $[M+Na]^+$) in the NP-HPLC–MALDI extracted ion chromatogram (Fig. 4b). These oligosaccharides eluted with a similar profile as the GH 11 DP 5 oligomers. However, MALDI-CID of the molecular ion signals spanning both peaks revealed that these structures are substituted with Ara*f* on Xyl*p* at the non-reducing end. The minor isomeric component gave high-energy fragment ions showing that Ara*f* is linked to the 3-position of non-reducing Xyl*p* and to C-3 of the middle Xyl*p* residue (Fig. 7a). In this case, the distributions of the Ara*f* residues along the xylan backbone are revealed by the important cross-ring fragment ions $^{1,5}X$ and $^{0,2}X$. The latter ions ($^{0,2}X_1$ and $^{0,2}X_2$) also show that both C-2 positions of the two backbone Xyl*p* residues are not linked to Ara*f*. This is supported by the ions E_2 and E_3 that are formed by elimination of OH from the C-2 position of Xyl*p* of their corresponding B_2 and B_3 ions. The presence of 3-linked Ara*f* on non-reducing Xyl*p* is revealed by the major G_3 ion at m/z 656.3. Importantly, this signal is absent in the fragment ion spectra of DP 5 GH 11 oligosaccharides, which contain unsubstituted Xyl*p* at the non-reducing end. This important G_3 fragment ion (m/z 656.3) is also present in the MALDI-CID spectrum of the major GH 10 DP 5 structural isomer (Fig. 7b) and indicates that Ara*f* is also linked to the 3-position of non-reducing Xyl*p* in this structure. However, other ions in this spectrum show that the non-reducing end Xyl*p* is disubstituted with Ara*f*. In particular, the dominant cross-ring fragments $^{1,5}X_2$ and $^{3,5}A_3$ indicate that the middle Xyl*p* is not linked to Ara*f*. Instead the minor $^{0,2}X_2$ ion (at m/z 600.3) suggests that Ara*f* is linked to the 2-position of non-reducing Xyl*p*. This is corroborated by major signals for E_2 (at m/z 271.3) and H_2 (at m/z 303.3) produced by elimination and cleavage of Ara*f* from the C-2 position of the B_2 and C_2 ions, respectively.

Inspection of the extracted ion chromatogram for DP 6 (m/z 954 $[M+Na]^+$) produced from xylanase GH 10 digestion (Fig. 4b) revealed four minor peaks, suggesting that this oligosaccharide has many isobaric components. Unfortunately, the molecular ion signals for these were too weak to obtain confident structural assignment by MALDI-CID. This is not unexpected, as a minor signal for DP 6 in the digestion mixture was also observed (Fig. 1b), suggesting that small

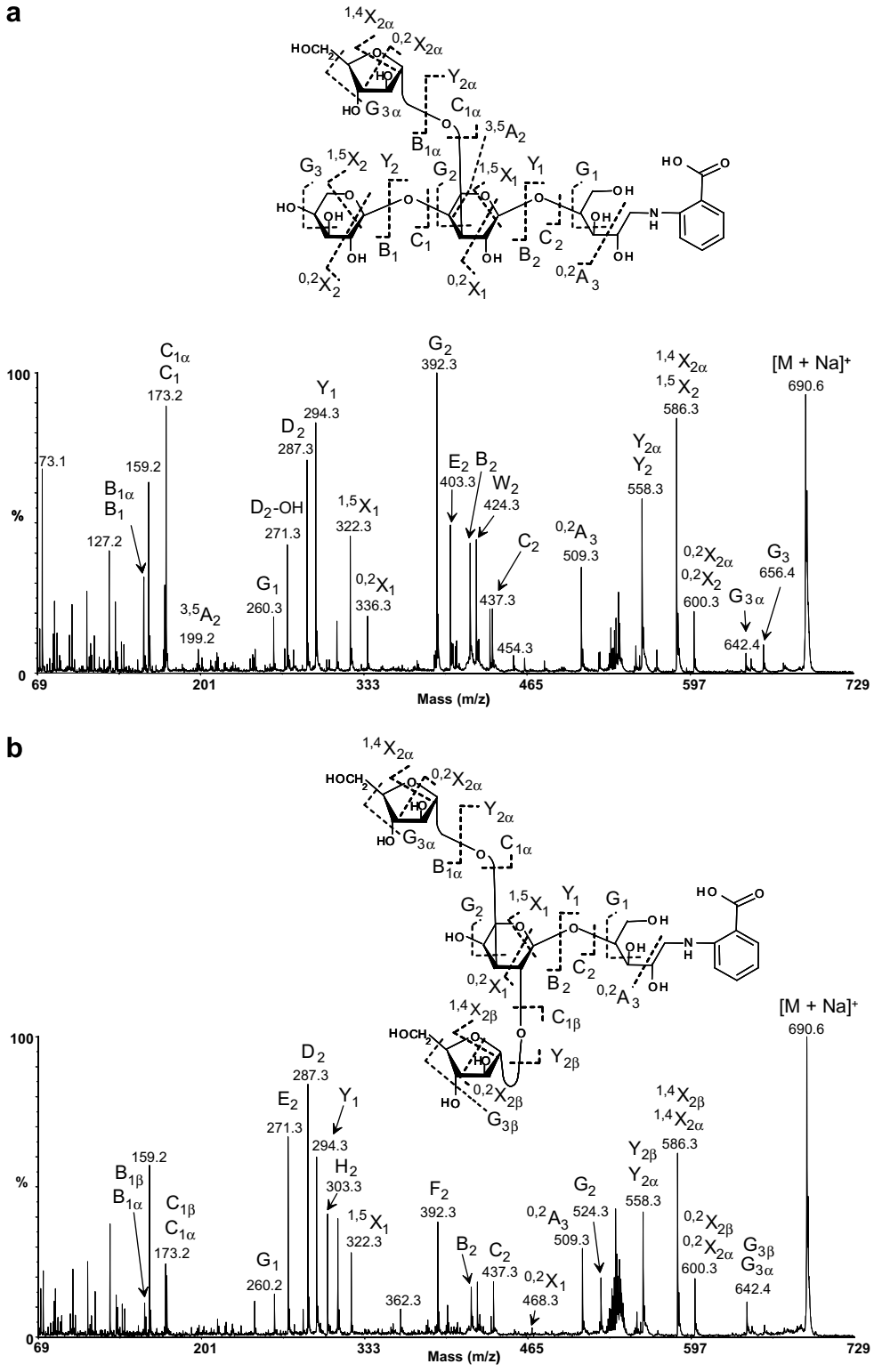

Figure 5. Chemical structures and accumulated NP-HPLC–MALDI-CID spectra of isomeric DP 4 AX oligosaccharides (*m/z* 690 $[M+Na]^+$) produced by digestion of the polysaccharide with endoxylanase from (a) GH family 11 and (b) GH family 10. Glycosidic and cross-ring fragments are labeled according to Domon and Costello nomenclature.[31] The proposed structures of the major ions denoted D, E, F, and G (nomenclature by Harvey[25] and Spina et al.[12]), H and W ions are summarized in Scheme 1.

amounts of this oligomer is produced by endoxylanase GH 10 digestion. By comparison, the GH 11 DP 6 oligosaccharides were represented by three significant peaks in the extracted ion chromatogram (Fig. 4a).

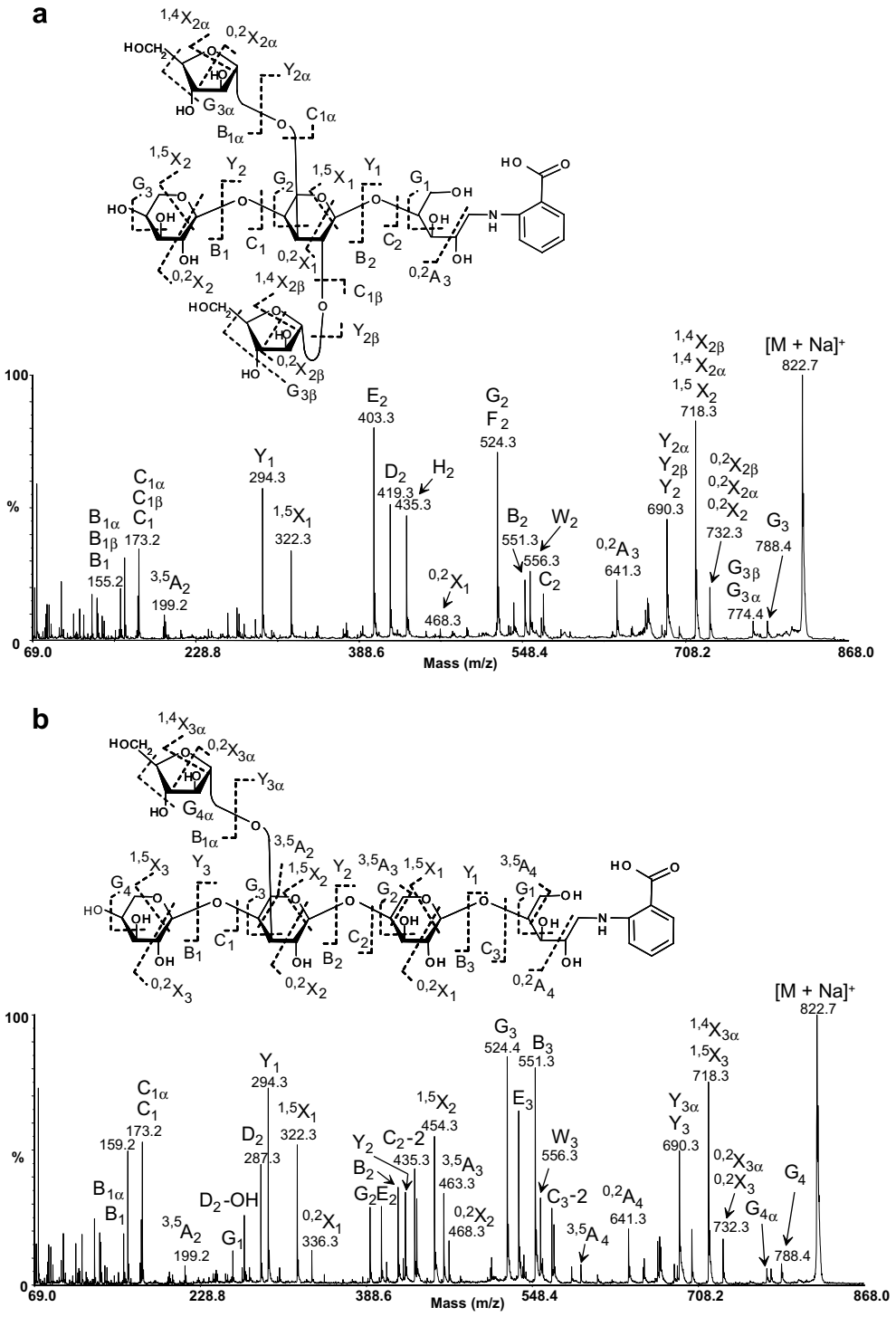

Figure 6. Chemical structures and accumulated NP-HPLC–MALDI-CID spectra of isomeric DP 5 AX oligosaccharides (*m*/*z* 822 $[M+Na]^+$) produced by digestion of the AX polysaccharide with endoxylanase from GH family 11. Glycosidic and cross-ring fragments are labeled according to Domon and Costello nomenclature.[31] The proposed structures of the major ions denoted D, E, F, and G (nomenclature by Harvey[25] and Spina et al.[12]), H and W ions are summarized in Scheme 1.

MALDI-CID of the structural isomer in the middle peak gave a fragment ion spectrum (data not shown) consistent with the DP 6 oligosaccharide standard shown in Figure 3b. Fragmentation of the first component in the extracted ion chromatogram of DP 6 revealed that this structure is composed of Xyl_4Ara_2 with the two Ara*f* residues 3-linked to each of the middle Xyl*p* residues (see Fig. 8). The MALDI-CID spectrum

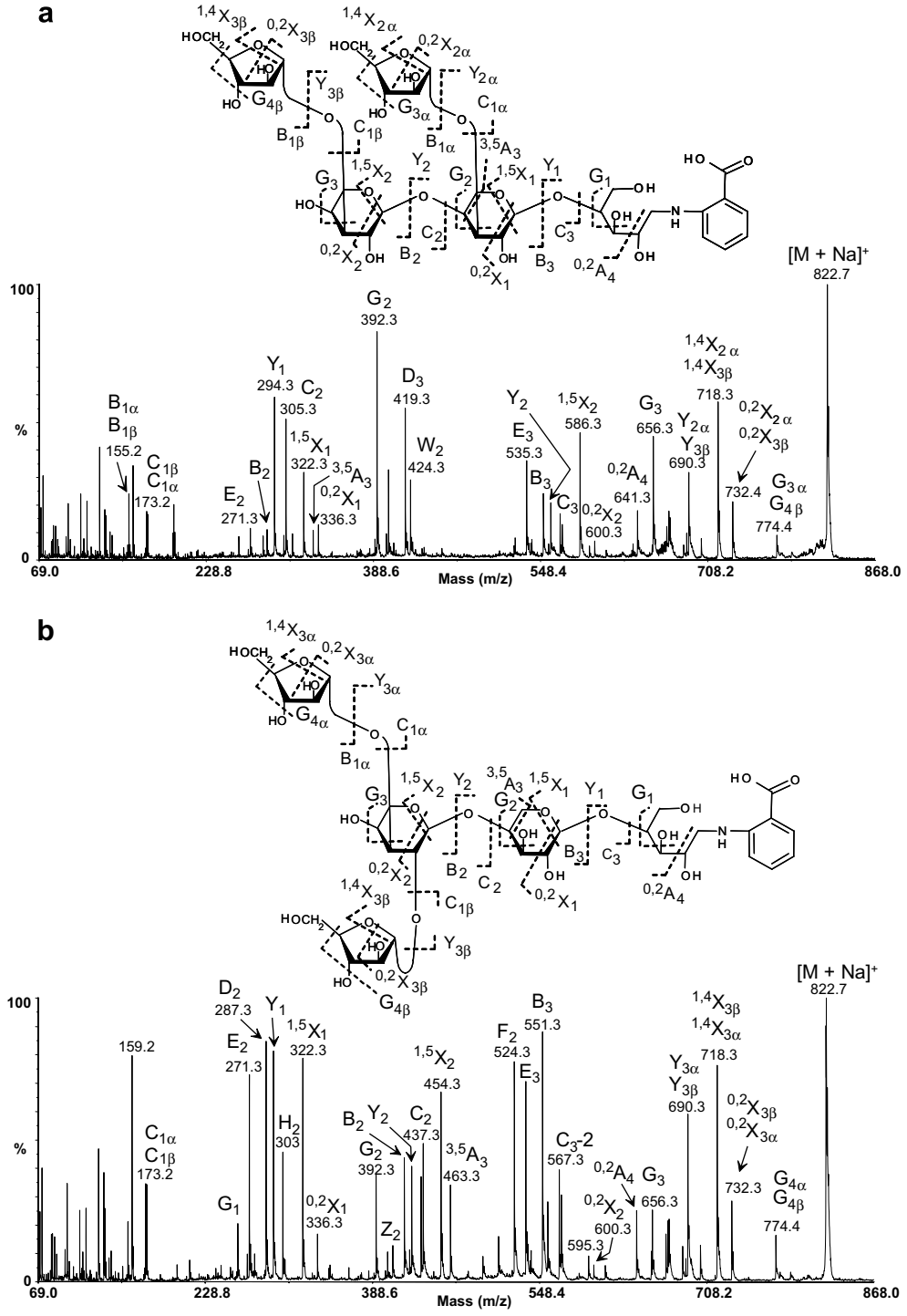

Figure 7. Chemical structures and accumulated NP-HPLC–MALDI-CID spectra of isomeric DP 5 AX oligosaccharides (*m/z* 822 $[M+Na]^+$) produced by digestion of the AX polysaccharide with endoxylanase from GH family 10. Glycosidic and cross-ring fragments are labeled according to Domon and Costello nomenclature.[31] The proposed structures of the major ions denoted D, E, F, and G (nomenclature by Harvey[25] and Spina et al.[12]), H and W ions are summarized in Scheme 1.

of the DP 6 oligomer in the last peak in the extracted ion chromatogram gave signals, which suggested that more than one isomer was present. These isobaric oligosaccharides are likely mixtures of monosubstituted AX that were not separated by the normal phase chromatography.

Similar structure elucidations were possible for some of the larger oligosaccharides produced by GH 11 diges-

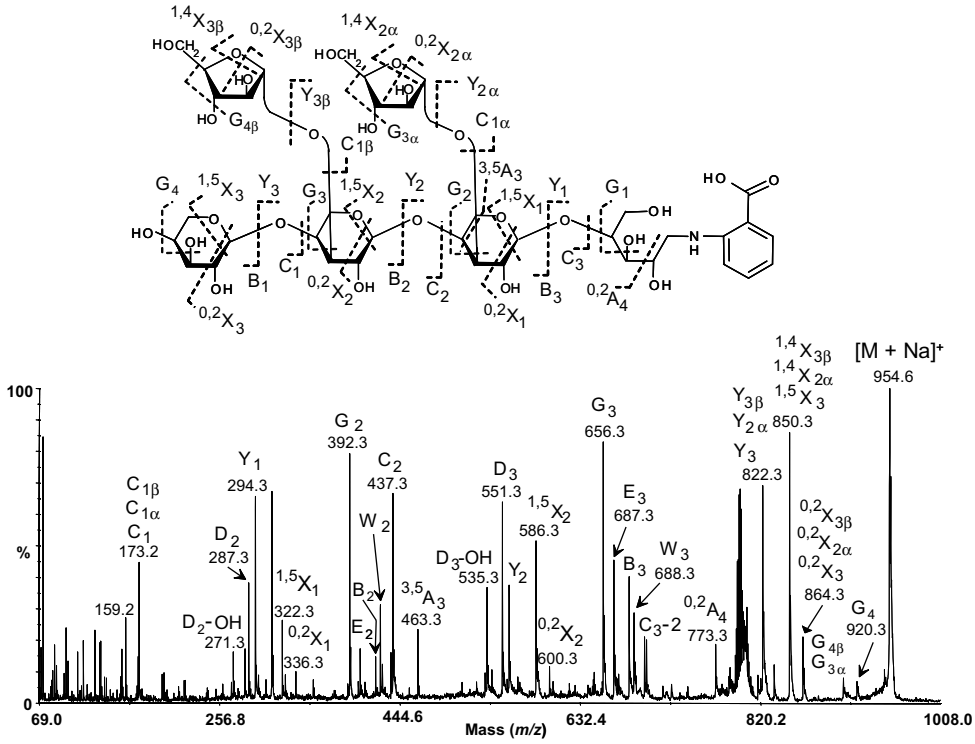

Figure 8. Chemical structure and accumulated NP-HPLC–MALDI-CID spectrum of an AX structural isomer (DP 6) produced from enzyme digestion of wheat AX with endoxylanase from GH family 11. Glycosidic and cross-ring fragments are labeled according to Domon and Costello nomenclature.[31]

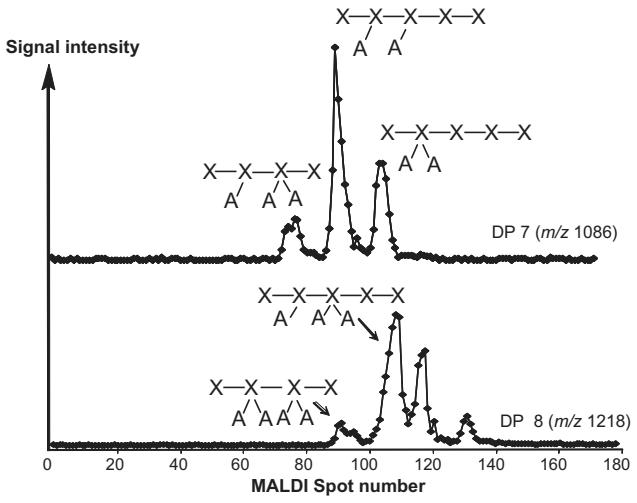

Figure 9. Extracted ion chromatograms showing isomeric oligosaccharides of DP 7 (*m*/*z* 1086 $[M+Na]^+$) and DP 8 (*m*/*z* 1218 $[M+Na]^+$) produced from enzyme digestion of wheat AX with endoxylanase from GH family 11. Oligosaccharide structures determined by MALDI-CID are indicated. Symbol representation of AX structure is: Ara*f*, A; Xyl*p*, X; (1→4) linkage, –; (1→3) linkage, /; (1→2) linkage, \.

tion (up to DP 8) (Fig. 9). However, complete characterization of all AX constituents from both GH 10 and GH 11 digestion proved too difficult due to the numerous structural isomers that arise.

Importantly, these structural data are consistent with the known specificities of these enzymes. Previous crystallographic studies have shown that GH 10 xylanases from *Cellvibrio mixtus*[26] (*Cm*Xyn10B) and *Streptomyces olivaceoviridis*[27] (*So*Xyl10A) can accommodate 2-linked methylated glucuronic acid (MeGlcA) at +1 but probably not the −2, −1 or +2 glycone site[26] (sugar-binding nomenclature according to Davies et al., with the cleavage occurring between subsites −1 and +1).[28] The MALDI data shown here indicate that 2-linked Ara*f* is accommodated in a similar manner to MeGlcA as this side chain is only observed at the non-reducing end (+1 subsite) of the GH 10 oligosaccharides studied. Previous crystallographic studies also revealed that both *Cm*Xyn10B and *So*Xyl10A enzymes can accommodate Ara*f* side chains linked to O-3 at −2, −3, and +1 subsites, but only *So*Xyn10A tolerated 3-linked Ara*f* at +2. The structural data presented here are consistent with the latter enzyme (*So*Xyl10A) as 3-linked Ara*f* is found on non-reducing Xyl*p* (+1 subsite) and its neighboring Xyl*p* residue (+2 subsite). In addition, no Ara*f* side chains were detected on reducing-end Xyl*p* (−1 subsite). By comparison, oligosaccharides produced by digestion with the GH 11 enzyme contained unsubstituted Xyl*p* both at the non-reducing (+1 subsite) and non-reducing ends (−1 subsite). These structures are expected based on previous studies on xylanases from

GH family 11, which are only able to hydrolyze unsubstituted regions of xylan.[24]

In conclusion, the NP-HPLC–MALDI-TOF/TOF method can facilitate the identification of distinct isobaric structures (DP 4–DP 8) produced by digestion of AX with different endoxylanases rapidly and with high sensitivity. Important structural information regarding the distribution of the Ara*f* side chains and extensive linkage information can be obtained using this off-line technique. However, owing to the complexity of the sample mixtures analyzed in this work, the comprehensive structural characterization of the larger isomeric oligosaccharides (DP 6–8) will require an additional fractionation step (e.g., high-pH anion exchange chromatography) prior to MALDI-TOF/TOF tandem MS. Despite this limitation, the results presented here show that this is a relevant technique for the detailed structure elucidation of isomeric mixtures of digested arabinoxylan and can be employed to understand the specificities of different endoxylanases.

3. Experimental

3.1. Preparation of oligosaccharides samples

Dextran 10 and wheat AX of medium viscosity were purchased from Sigma and Megazyme, respectively. The standard AX oligosaccharides were a gift (Dr. Luc Saulnier, INRA de Nantes, France). A dextran ladder was prepared by incubating dextran 10 in 200 μL 0.1 M TFA for 60 min at 100 °C followed by lyophilization. Wheat AX (0.5 mg) was digested with *Cellvibrio japonicus* xylanase Xyl10A from GH 10 or *Neocallimastix patriciarum* xylanase Xyl11A from GH 11[29] (gift from Prof Harry Gilbert, University of Newcastle, UK) in 0.1 M ammonium acetate pH 6 at room temperature for 14 h. The xylanases were inactivated for 30 min at 100 °C. The samples were filtered using Nanosep system (molecular weight cut-off of 10 kDa, Pall, New York, USA) and dried. The oligosaccharides were desalted using HyperSep Hypercarb cartridges (Thermo-Hypersil-Keystone, Runcorn, Cheshire, UK) as follows: prior to use, the columns were washed three times with 500 μL 80% (v/v) MeCN in 0.1% (v/v) TFA followed by three washes with 500 μL water. The samples were diluted with water to a final volume of 200 μL before loading onto the cartridges. The loaded cartridges were washed rigorously with water and 5% (v/v) MeCN containing 0.1% (v/v) TFA. Oligosaccharides were eluted with 3×200 μL of 50% (v/v) MeCN containing 0.1% (v/v) TFA and dried in a Speed Vac concentrator. The dextran polymer and AX oligosaccharides were reductively aminated with 2-aminobenzamide (2-AB) and 2-aminobenzoic acid (2-AA), respectively, using optimized labeling conditions described previously.[30] The saccharides were then purified from the reductive amination reagents using a GlycoClean S cartridge (Prozyme, San Leandro, CA). The GlycoClean S cartridges were washed with 1 mL water, followed by 5 mL 30% acetic acid, followed by 1 mL MeCN. Then the labeled oligosaccharides were applied to the disc and allowed to adsorb for 15 min, followed by addition of 100 μL MeCN, which was used to rinse the corresponding vial. Each cartridge was washed with 1 mL MeCN, followed by 5×1 mL 96% MeCN/water (v:v). The remaining oligosaccharides were eluted by washing with 3×0.5 mL water, followed by freeze drying.

3.2. NP-LC–HPLC–MALDI-TOF/TOF-MS/MS

NP capillary HPLC was carried out using a LC-Packings Ultimate System (Dionex, Sunnyvale, CA), which was used to generate the gradient that flowed at 3 μL min^{-1}. Solvent A was 50 mM ammonium formate adjusted to pH 4.4 with formic acid. Solvent B was 20% solvent A in MeCN. The labeled oligosaccharides (approx. 2 μg of AX digest and 100 pmol of 2-AB labeled dextran standard), dissolved in 80% MeCN, were loaded onto an amide-80 column (300 μm × 15 cm; Dionex, Sunnyvale, CA) and eluted with increasing aqueous concentration. For elution of AX oligosaccharides, the NP column was equilibrated at 5% A and the aqueous gradient was initiated 5 min after injection and increased linearly to 52% A over 131 min. The column effluent passed through a capillary UV detector (set at 254 nm for detection of both 2-AA and 2-AB oligosaccharides) directly to a Probot sample fraction system (Dionex, Sunnyvale, CA). This facilitated automated spotting of the HPLC eluent onto a MALDI plate (initiated 15 min after injection) at 20 s intervals (e.g., 1 μL/spot). After air drying, the sample spots were overlaid with 0.6 μL of 2,5-DHB (dissolved in 50% MeOH) and rapidly dried in a vacuum dessicator in order to produce small crystals for easy automated spectral acquisition. All mass spectra were recorded on a 4700 Proteomics Analyzer (Applied Biosystems, Foster City, CA). This MALDI tandem mass spectrometer uses a 200 Hz frequency-triple Nd-YAG laser operating at a wavelength of 355 nm. Averages of 1500 shots were used to obtain the MS spectra in automatic mode. Oligosaccharide molecular ions $[M+Na]^+$ were identified in the MALDI data and their elution positions in NP-HPLC were determined by carrying out an extracted ion chromatogram. Molecular ion signals $[M+Na]^+$ in every MALDI spot were selected for MALDI-CID in search of structural isomers. High-energy CID spectra were acquired manually with an average of 5000 laser shots/spectrum. The collision energy was set at 1 kV and the oligosaccharide ions were collided in the CID cell with argon at a pressure of 2×10^{-6} Torr.

Acknowledgements

The authors thank Professor Carol Robinson for her guidance and support and Professor Dudley Williams for helpful discussions. We thank Professor Harry Gilbert and Dr. Luc Saulnier for the gift of the endoxylanases and AX oligosaccharide standards, respectively. This work was supported by the BBSRC.

References

1. Izydorczyk, M. S.; Biliaderis, C. G. *Carbohydr. Polym.* **1995**, *28*, 33–48.
2. Kormelink, F. J. M.; Hoffmann, R. A.; Gruppen, H.; Voragen, A. G. J.; Kamerling, J. P.; Vliegenthart, J. F. G. *Carbohydr. Res.* **1993**, *249*, 369–382.
3. Gruppen, H.; Hoffmann, R. A.; Kormelink, F. J. M.; Voragen, A. G. J.; Kamerling, J. P.; Vliegenhart, J. F. G. *Carbohydr. Res.* **1992**, *233*, 45–64.
4. Vietor, R. J. H. R. A.; Hoffmann, R. A.; Angelino, S. A. G. F.; Voragen, A. G. J.; Kamerling, J. P.; Vliegenhart, J. F. G. *Carbohydr. Res.* **1994**, *254*, 245–255.
5. Broberg, A.; Thomsen, K. K.; Duus, J. Ø. *Carbohydr. Res.* **2000**, *328*, 375–382.
6. Hoffmann, R. A.; Leeflang, B. R.; Debarse, M. M. J.; Kamerling, J. P.; Vliegenthart, J. F. G. *Carbohydr. Res.* **1991**, *221*, 63–81.
7. Hoffmann, R. A.; Geijtenbeek, K. T.; Kamerling, J. P.; Vliegenthart, J. F. G. *Carbohydr. Res.* **1992**, *223*, 19–44.
8. Matamoros Fernández, L. E.; Obel, N.; Scheller, H. V.; Roepstorff, P. *J. Mass Spectrom.* **2003**, *38*, 427–437.
9. Matamoros Fernández, L. E.; Obel, N.; Scheller, H. V.; Roepstorff, P. *Carbohydr. Res.* **2004**, *339*, 655–664.
10. Quéméner, B.; Ordaz-Ortiz, J. J.; Saulmier, L. *Carbohydr. Res.* **2006**, *341*, 1834–1847.
11. Mechref, Y.; Novotny, M. V.; Krishnan, C. *Anal. Chem.* **2003**, *75*, 4895–4903.
12. Spina, E.; Sturiale, L.; Romeo, D.; Impallomeni, G.; Garozzo, D.; Waidelich, D.; Glueckmann, M. *Rapid Commun. Mass Spectrom.* **2004**, *18*, 392–398.
13. Stephens, E.; Maslen, S. L.; Green, L. G.; Williams, D. H. *Anal. Chem.* **2004**, *76*, 2343–2354.
14. Wuhrer, M.; Deelder, A. M. *Anal. Chem.* **2005**, *77*, 6954–6959.
15. Stephens, E.; Sugars, J.; Maslen, S. L.; Williams, D. H.; Packman, L. C.; Ellar, D. J. *Eur. J. Biochem.* **2004**, *271*, 4241–4258.
16. Wuhrer, M.; Koeleman, C. A. M.; Hokke, C. H.; Deelder, A. M. *Int. J. Mass Spectrom.* **2004**, *232*, 51–57.
17. Wuhrer, M.; Koeleman, C. A. M.; Deelder, A. M.; Hokke, C. H. *Anal. Chem.* **2004**, *76*, 833–838.
18. Royle, L.; Roos, A.; Harvey, D. J.; Wormald, M. R.; van Gijlswijk-Janssen, D.; Redwan, E.-R. M.; Wilson, I. A.; Daha, M.; Dwek, R. A.; Rudd, P. M. *J. Biol. Chem.* **2003**, *278*, 20140–20153.
19. Charlwood, J.; Birrell, H.; Camilleri, P. *J. Chromatogr. B Biomed. Sci. Appl.* **1999**, *734*, 169–174.
20. Butler, M.; Quelhas, D.; Critchley, A. J.; Carchon, H.; Hebestreit, H. F.; Hibbert, R. G.; Vilarinho, L.; Teles, E.; Matthijs, G.; Schollen, E.; Argibay, P.; Harvey, D. J.; Dwek, R. A.; Jaeken, J.; Rudd, P. M. *Glycobiology* **2003**, *13*, 601–622.
21. Henrissat, B.; Bairoch, A. *Biochem. J.* **1993**, *293*, 781–788.
22. Henrissat, B. *Biochem. J.* **1991**, *280*, 309–316.
23. Nurizzo, D.; Nagy, T.; Glbert, H. J.; Davies, G. J. *Structure* **2002**, *10*, 547–556.
24. Biely, P.; Vršanská, M.; Tenkanen, M.; Kluepfel, D. *J. Biotechnol.* **1997**, *57*, 151–166.
25. Harvey, D. J. *Mass Spectrom. Rev.* **1999**, *18*, 349–450.
26. Pell, G.; Taylor, E. J.; Gloster, T. M.; Turkenburg, J. P.; Fontes, C. M.; Ferreira, L. M.; Nagy, T.; Clark, S. J.; Davies, G. J.; Gilbert, H. J. *J. Biol. Chem.* **2004**, *279*, 9597–9605.
27. Fujimoto, Z.; Kaneko, S.; Kuno, A.; Kobayashi, H.; Kusakabe, I.; Mizuno, H. *J. Biol. Chem.* **2004**, *279*, 9606–9614.
28. Davies, G. J.; Wilson, K. S.; Henrissat, B. *Biochem. J.* **1997**, *321*, 557–559.
29. Gilbert, H. J.; Hazlewood, G. P.; Laurie, J. I.; Orpin, C. G.; Xue, G. P. *Mol. Microbiol.* **1992**, *6*, 2065–2072.
30. Bigge, J. C.; Patel, T. P.; Bruce, J. A.; Goulding, P. N.; Charles, S. M.; Parekh, R. B. *Anal. Biochem.* **1995**, *230*, 229–238.
31. Domon, B.; Costello, C. E. *Glycoconjugate J.* **1988**, *5*, 397–409.